

On Localizing a Camera from a Single Image

Pradipta Ghosh

University of Southern California
pradiptg@usc.edu

Xiaochen Liu

University of Southern California
liu851@usc.edu

Hang Qiu

University of Southern California
hangqiu@usc.edu

Marcos A. M. Vieira

Universidade Federal de Minas Gerais
mmvieira@dcc.ufmg.br

Gaurav S. Sukhatme

University of Southern California
gaurav@usc.edu

Ramesh Govindan

University of Southern California
ramesh@usc.edu

Abstract

Public cameras often have limited metadata describing their attributes. A key missing attribute is the precise location of the camera, using which it is possible to precisely pinpoint the location of events seen in the camera. In this paper, we explore the following question: under what conditions is it possible to estimate the location of a camera from a *single image* taken by the camera? We show that, using a judicious combination of projective geometry, neural networks, and crowd-sourced annotations from human workers, it is possible to position 95% of the images in our test data set to within 12 m. This performance is two orders of magnitude better than PoseNet, a state-of-the-art neural network that, when trained on a large corpus of images in an area, can estimate the pose of a single image. Finally, we show that the camera’s inferred position and intrinsic parameters can help design a number of *virtual sensors*, all of which are reasonably accurate.

1 Introduction

In the era of millions of smart devices and of emerging smart cities, the camera has become the most ubiquitous sensor deployed on the planet. With its ability to capture images and videos, it can obtain more detail about an environment than almost any other sensor can. As a result, in today’s world, there exist many cameras in a typical city like Los Angeles, San Francisco, and New York; a simple web search yields lists of hundreds of these cameras [1–3]. In a smart city environment, one can envision using these cameras for personalized fine grain navigation [4] to overcome GPS errors, for providing fast multi-camera surveillance [5] for health care, police personnel, or disaster relief operations.

However, in order to leverage these cameras for such applications, it is important to have accurate meta-data about the camera such as its focal length, its resolution, and its *pose* (location and viewing direction). Unfortunately, even something as simple as the precise location of a camera is not documented in lists of public outdoor cameras [1–3]. Preliminary analysis reveals that more than 90% of these sources only have coarse location labels, which vary from city to street level.

The Problem. In this paper, we address the problem of localizing a camera. The problem of localizing and characterizing a camera

from the camera feed is often known in the robotics and vision community (§6) as the *camera-relocalization problem* [6]. In these communities, the problem arises in map construction [7–9], to estimate the pose of the camera that captures 2D or 3D imagery for constructing the map. Because of their reliance on special sensors, these approaches may not be suitable for surveillance cameras. More recent work has proposed training, using a database of images with known poses, a neural network for camera pose estimation [6]. This approach, too, does not generalize to localizing static surveillance cameras (§5) primarily because there exists no large-scale open-source database of images that captures the diversity of properties and pose in real-world surveillance cameras; for example, the Google street view dataset consists of images taken at the street level, while surveillance cameras are often mounted at different heights.

In this paper, we take a first step towards understanding camera properties in the wild. Our approach is *deliberately* minimalistic. We ask: *Under what conditions is it possible to estimate the location of a camera from a single image taken by the camera?* Of course, just given an image and no additional information, it is difficult to estimate the camera’s pose. However, there *is* information (such as a landmark or a road feature such as a street corner) in the image that a neural network or a human might be able to extract. That, together with information from map APIs, might plausibly be able to localize the camera. In this paper, we explore ***the smallest set of additional information needed to localize the camera to within meter-level accuracy, given just a single image.*** We have left to future work to understand how to leverage *multiple* images to improve camera localization; our results provide an upper bound that future work can attempt to improve.

Approach. To localize a camera from a single image, we adapt techniques from projective geometry (§2), and methodically develop a set of algorithms that combine these with a judicious combination of neural networks and crowd-tasking. We find that in order to estimate the camera location from a single image, we need to first solve for a total of eighteen unknowns corresponding to: five *intrinsic* properties of the camera including the focal length of the camera, the pixel dimensions of the image, and the location of the image’s principal point *i.e.*, image center; twelve unknowns corresponding to *extrinsic* properties such as position and the orientation of the camera (§3); and one special unknown corresponding to the homogeneous camera projection equation (§3). Solving these unknowns can provide us the relative location of the camera with respect to a reference point visible in the image. To get the mapping from

Research reported in this paper was sponsored in part by the Army Research Laboratory under Cooperative Agreement W911NF-17-2-0196. The views and conclusions contained in this document are those of the authors and should not be interpreted as representing the official policies, either expressed or implied, of the Army Research Laboratory or the U.S. Government. The U.S. Government is authorized to reproduce and distribute reprints for Government purposes notwithstanding any copyright notation here on.

the relative location to the absolute location, we need to know the absolute (*i.e.*, GPS) location of the reference point.

Contributions. Our paper makes three important contributions.

Camera Relative Position. To estimate the five unknown camera intrinsic parameters, we develop novel image annotation methods to permit the use of vanishing point detection techniques from projective geometry [10]. The vanishing point (VP) of an image refers to the point or direction in the image to which a set of parallel lines in the real world converges (Figure 1b). A set of three orthogonal vanishing points of the image can help estimate the camera intrinsic properties as well as the unknowns related to the orientation of the camera (§3). However, the task of finding three orthogonal vanishing is not a trivial one [11]. Automated approaches for this often either require some property of the camera to be known [12] or output a wrong set of orthogonal VPs. We propose an approach that uses annotations from human workers (using a programmable crowd-tasking platform[13]), which leverages human perception and the wisdom of the crowds to achieve better results than possible with automated methods.

Given the vanishing points, we propose a novel algorithm to estimate the camera’s extrinsic properties (position and orientation). This technique needs an annotation for the dimensions of an object visible in the image, such as a car (§3). For this, we explore a range of approaches including using a pre-trained model of neural network for object detection, standard object dimensions, or crowd-sourced annotations of the object. We further show that, having estimated all eighteen unknowns, we can estimate the relative location of the camera with respect to any pixel of the image that corresponds to a point on the earth surface.

Camera Absolute Position. To get the absolute position (*i.e.*, the GPS coordinate) of the camera, ideally, we need the GPS coordinate of one reference pixel point. However, it turns out (§4) that due to ambiguity in the direction between the image and the real world, this is insufficient: we need the GPS coordinates of at least two reference pixels (§4). Using the fact that coarse location tags are often available for public cameras, we explore two particular scenarios to obtain positions of reference pixels: (1) when the nearest road intersection to a camera is known, and (2) when a landmark building is visible in the image and can be uniquely identified. For these cases, we develop a complete characterization the solution quality; in each case, we are able to narrow down the absolute location to one of a small number of candidate positions.

Applications. Finally, we show that the camera pose and intrinsic parameter estimates can help develop a variety of novel *virtual sensors* using the camera (§3.3, §4.3). A *virtual scale* can measure lengths in the physical world from the camera (*e.g.*, the length of a road divider), a *virtual clinometer* can measure building height, and a *virtual radar* can track vehicle speed. Finally, a camera’s absolute location can help develop a *virtual guide* for visually-challenged pedestrians.

Evaluation. To evaluate our algorithms, we have developed a software tool called CamLoc (§5) which implements these algorithms, and have evaluated it on a representative dataset of 214 images. Our evaluation (§5) shows that CamLoc can estimate the relative position of the camera with less than 10 meters error in

position and less than 3 meters error in height in $\approx 95\%$ of the test cases. Moreover, CamLoc is 1-2 orders of magnitude better than PoseNet [6], a deep neural network for pose estimation. We further show that if the pixel to GPS mapping of two points are known, CamLoc can output the absolute location of the image with less than 12 meters error in 95% of the test cases. A careful analysis of the images with bad performance of CamLoc shows that the errors are due to bad annotations for VPs as a result of non-obvious three perpendicular directions. We further demonstrate that even in the presence of ambiguity in the available information, CamLoc’s output solution almost always contains a candidate location for the camera that is within 10 meters of the actual location of the camera. Finally, we demonstrate that CamLoc’s virtual sensors are, in general, accurate to within 10-15% with high percentile, suggesting that they can help with *triage* (*e.g.*, determine where to deploy more reliable speed sensors).

2 Background and Approach

In this section, we discuss background material on modeling cameras using projective geometry, then describe our overall approach.

Coordinate Systems. A point seen by a camera can be represented in three different coordinate systems: *world*, *camera*, and *pixel*. The camera coordinate system has its origin at the camera’s focal point with z -axis towards the camera’s optical axis and the x - y direction along the camera image plane (Figure 1a). The image plane is at a distance f from the camera origin along the z direction of the camera coordinate system. The pixel coordinate system lies on the image plane with origin at the top left corner of any image as illustrated in Figure 1a. Image pixel locations are always represented in pixel coordinates. The point where the optical axis intersects the image plane is the image center whose pixel coordinates are $[u_{ic} \ v_{ic}]^T$ and camera coordinates are $[0 \ 0 \ f]^T$.

Notation. We denote the concatenation of two matrices \mathbf{A} and \mathbf{B} with same number of rows by $[\mathbf{A} \ | \ \mathbf{B}]$. We also denote the concatenation of two column vectors \mathbf{a} and \mathbf{b} by $[\mathbf{a} \ || \ \mathbf{b}]$.

Modeling Cameras using Projective Geometry. Two matrices suffice to model any monocular camera: an *extrinsic matrix* and an *intrinsic matrix*. The extrinsic matrix $\mathbf{M} = [\mathbf{R} \ | \ \mathbf{T}]$ contains information about the camera’s position and orientation (roll, pitch, and yaw) with respect to the world coordinate system. \mathbf{R} and \mathbf{T} are the rotational and translation matrix of the camera, respectively. \mathbf{R} is a special orthogonal matrix such that $\mathbf{R}\mathbf{R}^T = \mathbf{I}_3$ where \mathbf{I}_3 is a 3×3 identity matrix. This implies $\mathbf{R}^{-1} = \mathbf{R}^T$. Given a point \mathbf{x}^w in the world coordinate system¹, we can determine its camera coordinates using:

$$\mathbf{x}^c = \mathbf{M} [\mathbf{x}^w \ || \ 1] \quad (1)$$

We call this the *camera projection equation*.

The intrinsic matrix \mathbf{K} projects a point with camera coordinates \mathbf{x}^c onto the image plane. It requires three parameters: (a) focal length f of the camera; (b) pixel width dp_x and height dp_y , the physical dimension of each pixel; and (c) the image center (described above). Then, to obtain the pixel coordinates \mathbf{x}^p of a point with

¹To be precise, $\mathbf{x}^w = [x^w \ y^w \ z^w]^T$

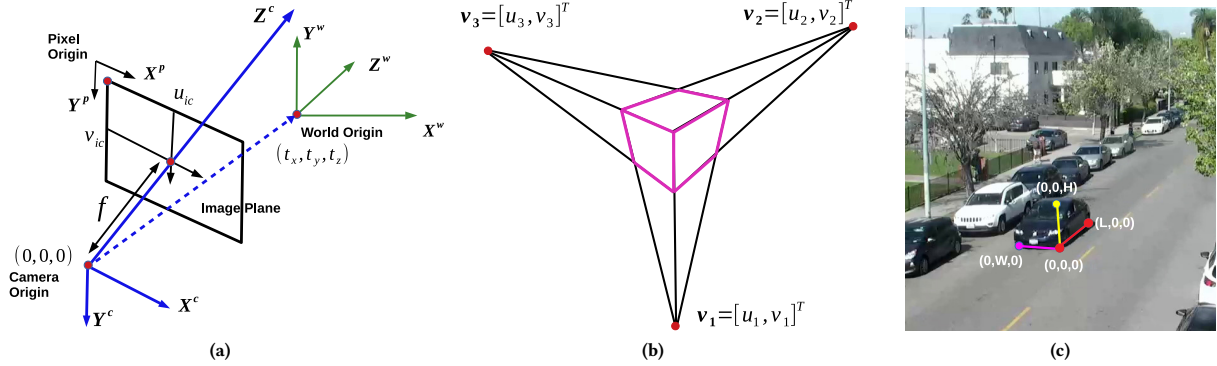


Figure 1: (a) Illustration of different coordinate systems. (b) Three orthogonal vanishing points for a right-angled cube. (c) Illustration of the world coordinate with the world origin at the nearest bottom corner of the car. L , W , H refer to the car's length, width, and height, respectively.

world coordinate \mathbf{x}^w , we use:

$$\lambda \begin{bmatrix} \mathbf{x}^p \\ 1 \end{bmatrix} = \mathbf{K}\mathbf{x}^c = \mathbf{K}\mathbf{M} \begin{bmatrix} \mathbf{x}^w \\ 1 \end{bmatrix} \quad (2)$$

We call this the *pixel projection* equation. λ is a constant used for homogeneous representation of the originally non-linear projection equation [14].

Vanishing Points. Our paper estimates the extrinsic and intrinsic matrices using the idea of *vanishing points*. Two parallel lines in the world coordinate system, when projected onto the image plane, appear to converge at a single finite *vanishing point*. However, if those lines are also parallel in the image plane, the vanishing point for those lines is at infinity. Two vanishing points are orthogonal if the parallel lines in the world coordinate system of one are perpendicular to the parallel lines of another. An image can have at most three mutually orthogonal vanishing points (Figure 1b) [15].

We use three properties of vanishing points to estimate the intrinsic and extrinsic matrices of a camera. (1) All lines in the same direction in the real world share the same vanishing point. (2) Given 3 finite orthogonal vanishing points (VP), the image center is the orthocenter of the triangle formed by the vanishing points. (3) Given 2 finite orthogonal vanishing points and one infinite vanishing point, one of the camera axis is parallel to one of the world axis.

Approach. In this paper, we explore techniques to determine both the *relative* (§3) and the *absolute* positions (§4) of a street-facing web-camera from which we have a single image. Clearly, using nothing else but the image, it is impossible to determine these positions, so we ask: What is the minimal set of additional contextual information necessary in order to accurately estimate these positions?

Our approach explores two types of contextual information: (a) image *annotations* obtained either through *crowd-sourcing* or using a trained *neural network*, (b) coarse absolute positions such as the nearest landmark or the nearest intersection.

Using these, we first estimate the vanishing points and use these to determine the extrinsic and intrinsic parameters of the camera (§3). Then, from the contextual information, we use absolute locations of landmarks or street corners to fix the absolute location of

the camera (§4). The following sections describe these contributions in greater detail.

3 Relative Localization

This section describes how we can estimate the relative position of a camera from a single image. First, we explain the theory underlying position estimation, some of which we have developed. This description identifies a *sufficient* set of annotations required to estimate the position. We then describe how we obtain these annotations.

3.1 Estimating Relative Position

Overview. We estimate the relative position with respect to world coordinates. So, the first annotation we need is to fix a point in the image as the world origin. Denote this by \mathbf{x}_O^w .

Then, to find the position of the world origin in the camera coordinate system, we can use the camera projection equation (Equation 1): $\mathbf{x}_O^c = \mathbf{M} \begin{bmatrix} \mathbf{x}_O^w \\ 1 \end{bmatrix}$. Now, the position of the camera in world coordinates is $-\mathbf{R}^T \mathbf{x}_O^c$ where \mathbf{R} is the camera rotational matrix (§2). But this requires the extrinsic matrix \mathbf{M} .

In practice, we can obtain the *pixel coordinates* \mathbf{x}_O^p of the world origin, for example, by a human selecting a specific pixel as the world origin. The camera coordinates of the world origin are, from Equation 2: $\lambda \begin{bmatrix} \mathbf{x}_O^p \\ 1 \end{bmatrix} = \mathbf{K}\mathbf{x}_O^c$. In this case, without knowing the intrinsic matrix \mathbf{K} and λ , we can not estimate \mathbf{x}_O^c .

To estimate the relative position, we need to solve for the extrinsic matrix \mathbf{M} and the intrinsic matrix \mathbf{K} by leveraging the pixel projection equation (Equation 2): $\lambda \begin{bmatrix} \mathbf{x}_O^p \\ 1 \end{bmatrix} = \mathbf{K}\mathbf{M} \begin{bmatrix} \mathbf{x}_O^w \\ 1 \end{bmatrix}$ (§2).

Thus, the key challenge in our work is to obtain the extrinsic matrix \mathbf{M} and the intrinsic matrix \mathbf{K} . Together, these matrices have the following unknowns: (a) Three unknowns each for roll, pitch, yaw, and translation; (b) The camera's focal length (f), the 2 pixel dimensions, and the pixel coordinates of the image center; and (c) The unknown constant, λ . However, λ is a function of the seventeen other unknowns mentioned above as well as the global coordinate of the point.

In the rest of this section, we show that, *with annotations from which we can extract the following pieces of information, we can estimate the extrinsic and intrinsic matrices, and therefore the camera’s relative position*. The required pieces of information are: (a) The world origin as well as three orthogonal axes defining the world coordinate system; (b) Three orthogonal vanishing points that correspond to the three axes direction of the world coordinate system. (c) The physical length of some object in the environment.

We first describe the mathematics underlying the estimation of these parameters, then discuss how we obtain these annotations.

Estimating the intrinsic matrix \mathbf{K} . Prior work [16] has described how to estimate the intrinsic parameters using a set of three orthogonal vanishing points, which we use directly. *Our contribution is the design of annotations to obtain a correct set of orthogonal vanishing points* (§3.2). We omit a description of this estimation for brevity.

Estimating the extrinsic matrix \mathbf{M} . The extrinsic matrix has two parts: the rotational matrix which we estimate using the vanishing points, and the translation matrix which we estimate using the world axes and the object dimension.

Rotational matrix. The rotational matrix consists of three vector components $\mathbf{R} = [\mathbf{r}_1 \ \mathbf{r}_2 \ \mathbf{r}_3]$. Let \mathbf{v}_i denote the i -th vanishing point $i \in \{1, 2, 3\}$. Then, we can use the estimated intrinsic matrix:

$$\lambda_i \mathbf{K}^{-1} [\mathbf{v}_i \ \parallel \ 1] = \mathbf{r}_i \quad (3)$$

This is because each direction of rotation (yaw, pitch and roll) corresponds to one vanishing direction.

To estimate the value of λ_i , we use the fact that $\|\mathbf{r}_i\|^2 = 1$ [17]. Using all three equations related to three vanishing points, we can estimate all three components of \mathbf{R} , modulo one important detail. A rotational matrix must satisfy two properties. In the singular value decomposition (SVD) of the rotational matrix $\mathbf{R} = \mathbf{U} \cdot \mathbf{S} \cdot \mathbf{V}^H$, \mathbf{S} should be an identity matrix. Moreover, the determinant of \mathbf{R} should be 1. Since the estimated rotational matrix \mathbf{R} might not satisfy these properties, we sanitize it using a standard SVD decomposition method from image processing [18].

Translation Matrix. We are now left with estimating the location of the world coordinate origin in the camera coordinate system, which is same as the camera’s translation matrix $\mathbf{T} = [t_x \ t_y \ t_z]^T$. For this, we need to fix the world coordinate origin $\mathbf{x}_O^w = [0 \ 0 \ 0]^T$. Let the corresponding pixel coordinate be $\mathbf{x}_O^p = [u_0 \ v_0]^T$.

To find \mathbf{T} , we need world coordinate of one other point. As we describe in 3.2, we obtain this from an image annotation: we leverage the fact that there exists, in surveillance cameras, objects with standard (or computable) physical dimensions, like a car (Figure 1c), human, or a common landmark (e.g., fire-hydrant). Let this second point be $\mathbf{x}_1^w = [L \ 0 \ 0]^T$, whose corresponding pixel coordinate is $\mathbf{x}_1^p = [u_1 \ v_1]^T$.

We can then write the following equations using the intrinsic and extrinsic matrices:

$$\begin{aligned} \lambda_0 \mathbf{K}^{-1} [\mathbf{x}_O^p \ \parallel \ 1] &= \mathbf{M} [\mathbf{x}_O^w \ \parallel \ 1] \\ \lambda_1 \mathbf{K}^{-1} [\mathbf{x}_1^p \ \parallel \ 1] &= \mathbf{M} [\mathbf{x}_1^w \ \parallel \ 1] \end{aligned} \quad (4)$$

From these two we get 6 equations to solve for five unknowns: three for \mathbf{T} and one for λ_0 and λ_1 each.

3.2 Obtaining the Annotations

For these estimations, we need three annotations in an image as discussed in §3.1: (1) world origin and axes, (2) three orthogonal vanishing points, and (3) one known dimension. We now describe how we obtain these annotations using deep neural networks (DNNs), and *when that is infeasible*, crowd-tasking on Amazon Mechanical Turk.

One known dimension. For this, we leverage the observation that street-surveillance cameras usually have one or more four wheeled vehicles (cars, trucks *etc.*) in their view. We first use an object detector to detect the vehicle, and then describe how we can estimate one of the dimensions of the vehicle.

Detecting vehicles. For this, we use a standard object detector DNN, SSD [19], which outputs bounding boxes as well as associated labels. However, for the next step in the annotation (described below), we need to find a vehicle (among those detected by SSD) whose three dimensions (length, width, and height) are fully visible. To do this, we leverage the observation that larger bounding boxes that are closer to the image center are likely to have the property we need. So, we pick that bounding box whose ratio of area to distance from the box center to the image center is highest.

Estimating car dimensions. For this, we use a pre-trained neural network [20] that, given a car image, outputs the car dimensions. Because this neural network is sometimes inaccurate, we also experiment with using fixed estimates for these dimensions (§5) based on the observation that most sedans have roughly the same size to within a meter or so.

Obtaining world origin and axes. For this, we use humans to annotate the four points shown in Figure 1c: the origin, and one point along each of the dimensions of the car. We use an image annotation crowd-sourcing service [13] for this purpose. This service enables users to programmatically submit tasks to annotate images (e.g., draw bounding boxes, track them, segment objects). It then automates the task of sending annotation requests to workers on Amazon Mechanical Turk (AMT) (called *Turkers*) and of collecting and curating results. We extended the service to incorporate our annotations. In our approach, the service sends each image, with the vehicle bounding box identified in the previous step, to multiple turkers. We describe below how we aggregate results from these Turkers.

Till date, we know of no *reliable* automated method for obtaining these annotations, which we have left it to future work.

Obtaining vanishing points. To determine a vanishing point, we need to find two lines in the image that are parallel in the real world (e.g., the sides of a rectangular building, the sides of a car). For our



Figure 2: (a) Web UI for annotation crowdsourcing. (b) Sample annotation collected. Red, purple, and yellow lines correspond to x-axis, y-axis, and z-axis in the world coordinate frame of reference. (c) Illustration of building height (left) and parking space annotation (right).

estimation to work (§3.1), we need these lines to align with the axes identified in the previous step.²

For this, we evaluate two approaches. In the first, we use the Canny edge detector to find all edgelets (small edges) in the image. Then we use the car axis directions and the RANSAC method [21] to filter out the edgelets that are not consistent with the world axis direction then estimate the three vanishing points using [12].

Because this method is sometimes unable to find three vanishing points, we use crowd-sourcing to obtain these annotations. In this method, the Turker is asked to draw 3-4 lines that are parallel to each of the car axis. We use the same service described above [13], and have extended the service to obtain vanishing point annotations.

Figure 2a shows the webpage the service presents to each Turker. Each Turker annotates the car axes and three sets of parallel lines. Figure 2b shows a sample result from a Turker, which depicts three sets of mutually orthogonal lines pertaining to the vanishing points.

Putting it all together: Robustly estimating the camera’s relative position. Our annotations are *minimal*: we *get just the information needed by the underlying mathematical framework*. From these annotations, we can estimate the intrinsic and extrinsic matrices, then obtain the camera’s relative position as discussed above. In practice, we may need to aggregate multiple *candidate locations* in order to get a robust position estimate. Since untrained Turkers may produce inaccurate results, we generate candidate locations from each worker’s annotations. Furthermore, since the car dimension estimator is sometimes erroneous, we obtain two different estimates of the translation matrix: one from the car’s length and the other from the car’s width. Thus, for each Turker, we get two candidate locations. We then cluster these locations by distance, and estimate the camera position by the centroid of the largest cluster.

3.3 Applications

Beyond estimating the relative position of the camera, we can estimate, under some conditions, the world coordinate \mathbf{x}^w corresponding to *any* given pixel coordinate \mathbf{x}^p . To do this, we can use the pixel projection equation (Equation 2): $\lambda [\mathbf{x}^p \parallel 1] = \mathbf{KM} [\mathbf{x}^w \parallel 1]$.

²As a matter of detail, the annotated vehicle need not be parallel to the street, but the annotations for the vanishing points must align with the car.

However, in this system, there are three equations with four unknowns λ and the three world coordinates.

Under some conditions, we can use this capability to *employ the camera as a virtual sensor*.

Virtual scale. Just as scales can measure dimensions, the camera’s position, together with human annotations, can be used to estimate lengths or distances. If a human could annotate a pixel on the ground plane (as shown in Figure 2c (right)), then there are only 3 unknowns (since the z-axis value is zero, assuming that the world coordinate system is on the ground plane as is the case with our annotations), so it is possible to obtain the world coordinate of this pixel using Equation 2. We show that, if a human annotates two pixels that demarcate the edges of some feature on the ground plane (e.g., a parking space or a road divider) we can estimate the length of this feature.

Virtual clinometer. A clinometer measures building height. Our approach can synthesize a virtual clinometer from the camera, as follows. If a human can annotate a pixel \mathbf{x}_1^p where a building’s face meets the ground, and a pixel \mathbf{x}_2^p at the top of the building vertically above \mathbf{x}_1^p (as illustrated in Figure 2c (left)), we can estimate the building height. This is because, since \mathbf{x}_1^p is on the ground, there are only 3 unknowns in estimating the world coordinate of \mathbf{x}_1^p . Once we know \mathbf{x}_1^p ’s world position, we can determine \mathbf{x}_2^p ’s since its *x* and *y* coordinates are the same as \mathbf{x}_1^p ’s. The Euclidean distance between these two points is the height of the building.

Virtual radar. A radar measures vehicle speeds. From a camera’s consecutive frames, we can obtain a cheap, but approximate, vehicle speed estimator. To do this, we use a feature based tracker such as KLT [22], which tracks image features across multiple frames. To estimate the speed, we estimate the distance traveled by a feature belonging to a car (δ) in successive frames and use the camera’s frame rate (*fps*) to estimate the speed ($\delta * fps * 3.6$ kmph).

4 Absolute Localization

Obtaining the absolute location of the camera (in terms of its latitude and longitude), given its relative location, is a significant challenge. As with relative location, we need additional contextual information to determine absolute location. In this section, we begin by describing how to determine absolute location using minimal

additional information, then discuss how to obtain this additional information in practice.

4.1 Estimating Absolute Position

Overview: The intrinsic and extrinsic matrices (§3.1) give us the world coordinates of the camera. Let \mathbf{x}_1^p be the pixel coordinate of a ground plane point. Using the pixel projection equation (Equation 2), we can obtain that point’s global coordinate, and, from that the relative position of the camera *with respect to that ground plane point*. Then, if we knew the absolute position of pixel \mathbf{x}_1^p , we can just use it to find the absolute position of the camera. To do this, we need to: (a) obtain the absolute position of the image pixel, and (b) the mapping between our world coordinates and the geodetic (latitude/longitude) coordinate system.

Given the absolute position of a pixel. Let (lat_1, lon_1) be the known absolute position of the pixel (§4.2 discusses how we can obtain this), and let d be the distance and α the bearing from that point to the camera. Then, prior work [23] provides the following approximation for small d (less than 1-2 kms, which holds for camera ranges) for the absolute position (lat_c, lon_c) of the camera:

$$\begin{aligned} lat_c &= lat_1 + (d \cdot \cos \alpha) / 111111 \\ lon_c &= lon_1 + (d \cdot \sin \alpha) / (111111 \cdot \cos(lat_1)) \end{aligned} \quad (5)$$

where the constant 111111 is the distance on the Earth’s surface corresponding to 1 degree change in latitude and α is the bearing (clockwise) towards the true north.

Estimating α : Public APIs for Google Maps and Open Street Maps provide the angle (clockwise) of the street θ relative to the true north. Now, suppose one of the world axes (say the x-axis) aligns with the direction of the street. Then, knowing the relative position of the camera, we can estimate the bearing of the camera, ϕ , relative to the pixel point in the world coordinates. From this, we can estimate α , the bearing of the camera relative to the pixel point in the geodetic system to be $\alpha = 90 + \phi + \theta$ (Figure 3a) where all the values are in degrees.

Unfortunately, there is still an important source of ambiguity: from the image, we cannot know which direction of the street the camera is facing. For example, if the street runs from southwest to northeast, the street’s bearing in that direction is 45 degrees, but in the opposite direction is 225 degrees. From this, we get two possible values for α . This arises because we don’t know how the world x and y axes relate to the geoidal directions. For each choice of bearing, there are two choices for the y-axis direction. This leads to four candidate locations for the camera when using (Equation 5), as shown in Figure 3b.

Given the absolute position of two pixels. In this case, it becomes easier to estimate the absolute position of the camera. From the pixel coordinates of the pixels, we can estimate the world coordinate locations of the pixels, and their distances (d_1 and d_2) to the camera. The camera must lie at one of the two points at which the circles centered at each pixel, with radius d_1 and d_2 respectively, intersect. We can find the absolute positions of these two points (using Equation 5). There still remains ambiguity in selecting one location.

A human annotator or a simple comparison of the pixel coordinates of the reference pixel can eliminate this ambiguity. In Figure 3c, \mathbf{x}_1^p and \mathbf{x}_2^p are the two pixels and \mathbf{x}_{c1}^w and \mathbf{x}_{c2}^w are the candidate locations. By examining the relative ordering of \mathbf{x}_1^p and \mathbf{x}_2^p when scanning the camera image from left to right, we can determine whether \mathbf{x}_{c1}^w or \mathbf{x}_{c2}^w is the correct absolute position. In our example, if \mathbf{x}_1^p is to the left of \mathbf{x}_2^p , \mathbf{x}_{c1}^w is the correct position, \mathbf{x}_{c2}^w otherwise.

4.2 Obtaining Absolute Position of Pixels

To obtain the absolute position, *we must have some coarse grain information about the camera’s location*.

Road Intersection. If we know the intersection near which the camera is located, and if at least one of the corners of that intersection is visible on the camera, we can narrow down the absolute location of the camera to a handful of candidates. For this, we rely on human annotation.

We present both the image and the satellite view of the respective road intersection to a human annotator as shown in Figure 4 and ask him/her to mark all the corners in both images in a *clockwise* manner. We then have an ordered list of visible corners in the image, and, using a map service, we can get the GPS coordinates of each intersection point.

This leads to another ambiguity: it is impossible for a human operator (without additional information) to identify which corner in the image corresponds to which corner in the satellite view. This ambiguity results in candidate positions whose number depends on the number of corners visible in the camera image.

One visible corner: If only one corner is visible, it can map to one of the 4 corners in the satellite image. For each of these points, we get 4 candidate locations (§4.1), resulting in 16 candidates for the absolute location. We have assumed that the intersection has only four corners; our analysis can be extended to more complex intersections.

Two visible corners: With two visible (adjacent) corners, there are 8 possible mappings between these and the four corners in the satellite view. This results in 8 candidate solutions (for each choice, we can exactly pinpoint the location, §4.1). We can narrow these down further as follows. We first estimate the distance between the two visible corners using the method discussed in §3.2 for finding dimensions in an image. From the absolute positions of the corners obtained from the satellite view, we can also find the distances between the intersection corner points. We can match the image distance to the closest satellite view distance. This works well when two streets of different widths intersect. In this case, we can reduce the number of candidates to two (Figure 4) by symmetry.

More than 2 visible corners. With 3 or 4 visible corners, we can use similar matching techniques: in this case, we would match the sequence of distances between successive corners (assuming that the corner annotations are clockwise). Even so, however, because



Figure 3: (a) Illustration of different components of the absolute position estimation. (δ_x^w, δ_y^w) is the estimated position of the camera relative to the landmark pixel. (b) Candidate locations based on one reference point. The yellow marker is the actual camera location. Red markers are the estimated camera location candidates. (c) Estimating a unique camera location using two pixel-to-GPS mappings.



Figure 4: Two-corner-based absolute position estimation. The top two pairs of candidate positions are illustrated as in red and green, respectively.

intersections are symmetric, there are always at least two candidate matches for any sequence of corner distances, so we cannot completely eliminate the ambiguity.

Landmark Building. If the camera is near a known landmark building (such as a restaurant or a retail store) whose GPS location is available using a map API, and the landmark is also visible in the camera, then we can get some candidate absolute positions in at least two ways: asking the human to annotate a *building corner* or the mid-point of the *building face* and assuming that annotated pixel’s GPS location is the same as the building’s. In either case, similar ambiguities exist as with using road corners; we omit the details of this estimation for brevity, but present results in §5 to show how well this approach works.

4.3 Applications

Using these annotations, we can estimate the camera’s absolute position as described in §4.1. From this, we can estimate the absolute position of any ground pixel in the image.

Virtual guide. Using this, we can track a person appearing in an image whose GPS trace is approximately known, a capability we call a *virtual guide*. This can provide navigation guidance for visually-challenged users. Suppose such a user has a cellphone that continuously updates a cloud service with its own location. The cloud service can, using a nearby camera, estimate where the person is on the camera (because it can obtain the pixel position of the user’s GPS location), then alert the user to obstacles on the way (e.g., fire hydrants, objects on the sidewalk etc.). In practice, because GPS locations can be inaccurate, the cloud service will need

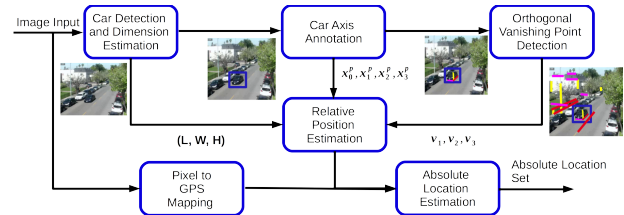


Figure 5: CamLoc workflow

to (a) use a DNN to detect bounding boxes for the person, and *track* their absolute positions over time (by converting successive pixel positions to absolute positions) and (b) *match* the tracks with the GPS tracks. To do this tracking robustly in the presence of multiple users, we use a technique from Liu et al. [24].

5 Evaluation

In this section, we evaluate relative and absolute position accuracy using a custom dataset containing 214 images, and compare its performance against PoseNet [6], a state-of-the-art Deep Neural Network for camera localization.

5.1 Methodology

Implementation. We have instantiated our algorithms into an end to end system, called CamLoc, which has six components as shown in Figure 5. The *Car Detection and Dimension Estimation* component takes the camera image as input, outputs the 2D bounding of the most-visible car along with its three dimensions (L, H, W). For estimating dimensions, CamLoc uses standard sedan dimensions. *Car Axis Annotation* uses crowdsourcing to obtain the world origin and the three world axes (Figure 1c). *Orthogonal Vanishing Point Detection* extracts the three orthogonal vanishing directions using crowdsourced annotations. *Relative Position Estimation* uses the techniques described in §3 to estimate the relative position of the camera, while *Pixel to GPS Mapping* obtains pixel annotations using crowdsourcing (§4.2). Finally, *Absolute Location Estimation* outputs the candidate absolute positions using techniques described in §4. Overall, CamLoc requires 1,680 lines of code in Python.

Dataset. CamLoc localizes a camera from a single image taken by the camera. We were unable to find an open-source image database with ground-truth locations and having the diversity of camera

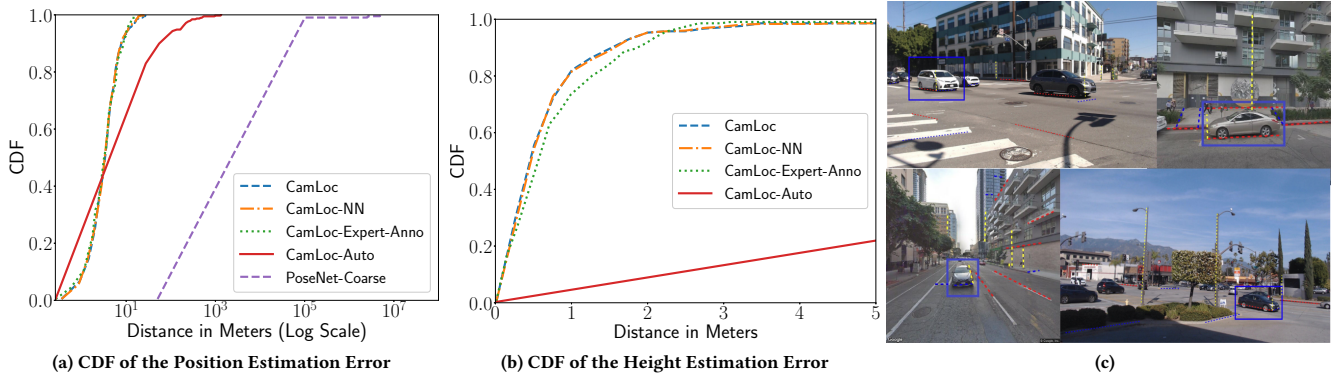


Figure 6: (a, b) Relative position error analysis, (c) Four sample images that are hard to annotate. The top-left image contains a corner where intersecting roads are not perpendicular. For the rest three images, one of the dimension is not too apparent at first look.

poses, camera parameters, and image quality in surveillance cameras. Google Street View provides some diversity and ground truth, but all images are at street level from cameras with identical properties. To have more diversity, we use a dataset of 214 images in which roughly 50% of the images are from Google Street Views. Another 40% of the images we collected using smartphone cameras from roughly 80 different combinations of locations, pose and elevations around a large city in North America. The remaining 10% are snapshots from different public online cameras such as EarthCam and three campus surveillance cameras in the same city.³ Our dataset also has, by design, diversity in image resolution; despite this, as we show below, CamLoc is able to estimate camera position well.

Ground Truth. For our evaluations, we annotated, using a tool we developed, the ground truth GPS location of the camera and the selected car in each image along with the relative location. Our annotation tool combines GPS measurement, satellite views, and human-in-the-loop to output the ground truth. We also use this annotation tool to obtain ground truth for our applications.

Comparison. We compare the performance of CamLoc with PoseNet [6]. To this end, *we trained PoseNet on the Street View dataset of a large metropolis containing 368,000 images* totaling up to 24 GB. Further, to compare how PoseNet performs when we have more context for the absolute location and can narrow the search space to a smaller region, *we retrain PoseNet on a much smaller dataset that contains 74,000 street view images from our campus neighborhood.* We refer to these two separate models as *PoseNet-Coarse* and *PoseNet-Fine*, respectively.⁴

To illustrate the impact of our design choices for some of the components, we also compare CamLoc with the following alternatives: *CamLoc-NN* uses a pre-trained neural net to detect vehicle dimensions; *CamLoc-Auto* uses an automated approach to detect

vanishing directions [12]; and *CamLoc-Expert-Anno* uses annotations by an expert to understand the efficacy of crowdsourcing.

Experimental setup. The experiments run on an Intel Core i7 8700 CPU @ 3.20GHz×12 machine with GeForce GTX 1050 Ti GPU.

5.2 Relative Positioning Accuracy

In this section, we evaluate the relative localization performance of CamLoc system. We compare CamLoc with different variants of CamLoc and *PoseNet-Coarse*. PoseNet outputs the absolute position of the camera. For the purpose of comparison, we convert this to the relative position with respect to the world origin using the camera projection equation (Equation 1).

Position Estimation Error. In Figure 6a, we compare the error in the relative position estimation in meters between the estimated location and the ground truth location. The relative position error in CamLoc is less than 5 meters for $\approx 80\%$ of the images and less than 10 meters for 95% of the images. A careful analysis of the images reveals that errors larger than 5 m occur when one dimension of the car/environment is not visible or unclear. This results in the human annotator not being able to draw parallel lines correctly, so CamLoc is unable to determine three vanishing points. We show four examples of such images in Figure 6c. The other prevalent reason for the high error is that Turkers annotate the wrong car corner as the world origin (we ask them to annotate the corner closest to the camera). This can lead to an error up to the length of the car $\approx 4.5m$.

CamLoc outperforms PoseNet. Figure 6a clearly demonstrates that CamLoc outperforms PoseNet *by nearly 2 orders of magnitude*. When trained over a corpus of images in a large area, PoseNet loses the ability to precisely match images and determine pose. Two factors account for the discrepancy between the sub-meter localization error presented in its original evaluation [6]. First, the *testing and training images* in PoseNet’s original evaluation *use the same camera* at a relatively consistent height. In contrast, our training images use Google Streetview images taken at street level but our test images are from multiple surveillance cameras, smartphones, and webcams with different camera properties from a wide

³We plan to make the dataset publicly available upon publication.

⁴Recent research has improved PoseNet; we describe why we do not compare against these in §6.

range of heights and orientations. PoseNet is unable to generalize well to these. Second, the evaluation in [6] *uses images taken from a few hundred meters stretch of road, much smaller in scope than our city-wide training dataset* (tens of square kms). At these larger scales, Posenet is unable to effectively extract features unique to specific camera poses, leading to inferior performance. By contrast, CamLoc uses precise geometric techniques, together with human annotations tailored towards the specific image, in order to determine relative position.

CamLoc is better than other variants. CamLoc outperforms CamLoc-Auto in the tail by an order of magnitude. Automated vanishing point detection can fail to find three vanishing directions in situations where human annotators are able to find these (we discuss this in more detail below). CamLoc-Expert-Anno, with annotations from an expert, performs almost the same as CamLoc which incorporates annotations from multiple untrained turkers. This is likely due to the “wisdom of the crowds” phenomenon; the aggregated results from multiple untrained workers have been repeatedly shown to match ground truth well. Finally, CamLoc-NN, which uses a neural net to estimate car dimensions, does not perform appreciably better than CamLoc; this suggests that it might be sufficient to use standard dimensions for this component.

Camera Height Estimation Error. From its relative position estimates, we explore how well CamLoc can estimate camera height (Figure 6b). In this experiment, we do not compare CamLoc with PoseNet, since the latter is trained on Street View images all taken from the same height.

CamLoc estimates camera height better than alternatives. Figure 6b shows that CamLoc with human-in-the-loop can achieve less than 1 m error in height estimation for 80% of the test images and less than 3 m error in 95% of the cases. CamLoc-Auto performs the worst. As with position error, errors higher than 1 m occur when at least one dimension of the car/environment is not visible/prominent, as illustrated in Figure 6c.

Why CamLoc-Auto performs poorly. While automated detection of the most promising vanishing point can be very accurate, detecting the second and third orthogonal vanishing point is very challenging with automated line detection and grouping of parallel lines. Often the automated approach outputs three vanishing points that are not orthogonal at all. In cases where the system is able to detect a set of orthogonal vanishing points, it most often does not align well with the car axes and therefore can not leverage the car dimensions to estimate the camera location. This is exactly what led us to design crowd-sourced annotations for vanishing points.

5.3 Absolute Positioning Accuracy

In this section, we analyze the error in absolute position estimation. For this, we perform three sets of experiments as described below.

Two Known Points. In the first set of experiments, we get the pixel to GPS mapping for two pixels by leveraging a combination of landmark location, road intersections, and different features on the road such as a left-turn arrow or stop sign text. From these, we extract the absolute positions of two pixels and compare CamLoc against four variants and PoseNet-Coarse.

In this experiment, we also ask: would PoseNet perform better if its models were geographically specialized? That is, if we knew the precise area covered by a set of cameras, and we trained PoseNet with images only from that area, would it perform better? For this, we compare CamLoc against PoseNet-Fine (§5.1).

CamLoc outperforms other alternatives. Figure 7a clearly shows that CamLoc with human annotations can achieve less than 12 meters errors for 95% of the images. This performance is consistent with the relative position error performance of CamLoc. Both variants of PoseNet perform really poorly on the test images with errors that are one or two orders of magnitude worse than CamLoc. While PoseNet-Fine performs slightly better than PoseNet-Coarse, it is still an order of magnitude worse than CamLoc. The performance of CamLoc-Auto is also much worse than CamLoc again due to either not being able to detect three orthogonal vanishing points or detecting a set of orthogonal vanishing points that are not aligned with the car axes.

For relative positioning, CamLoc was comparable to CamLoc-NN and Camloc-Expert-Anno. However, for absolute positioning, it is better than these two alternatives. CamLoc is better than CamLoc-Expert-Anno because the wisdom of the crowds has a stronger effect in this case, where the turkers are able to collectively annotate pixel to GPS mappings better. CamLoc outperforms CamLoc-NN since the latter inconsistently and inaccurately estimates car dimensions across multiple runs. In summary, for the case with known mapping of two ground pixels with their GPS location, CamLoc can achieve localization accuracy in the order of a few meters, comparable to GPS error in congested city environments.

We do not report height estimation error since that is the same both with absolute and relative positions.

Road Corners. We now consider a more restrictive case, when the only available information is that the camera is near a known intersection and the corresponding road corners are visible in the image. For this set of experiments, we handpicked a set of 50 representative images where the road intersections are visible. In this setting, recall that CamLoc outputs multiple candidate locations.

Figure 7b plots the CDF of the distance to the closest candidate location output of CamLoc as well as the distance to the furthest candidate location from the ground truth location. The closest candidate location is within 10 m of the actual location for almost more than 80% of the test cases and within 15 m for 100% of the test cases while the furthest candidate is sometimes 100 m away. Even the furthest candidate location is orders of magnitude closer to the ground truth than the PoseNet-Coarse and PoseNet-Fine.

Landmark Building. In this section, we present CamLoc performance for the case when a landmark building is visible in the image. As discussed in §4.2, CamLoc can use two annotations: landmark midpoint annotation on the most prominent visible face, or annotations on visible corners. In our experiments, we use both of these methods and obtain a set of candidate locations from them.

Figure 7c plots the minimum and maximum distance of the candidate locations from the ground truth location for both cases. With corner annotations, CamLoc output always contains a candidate

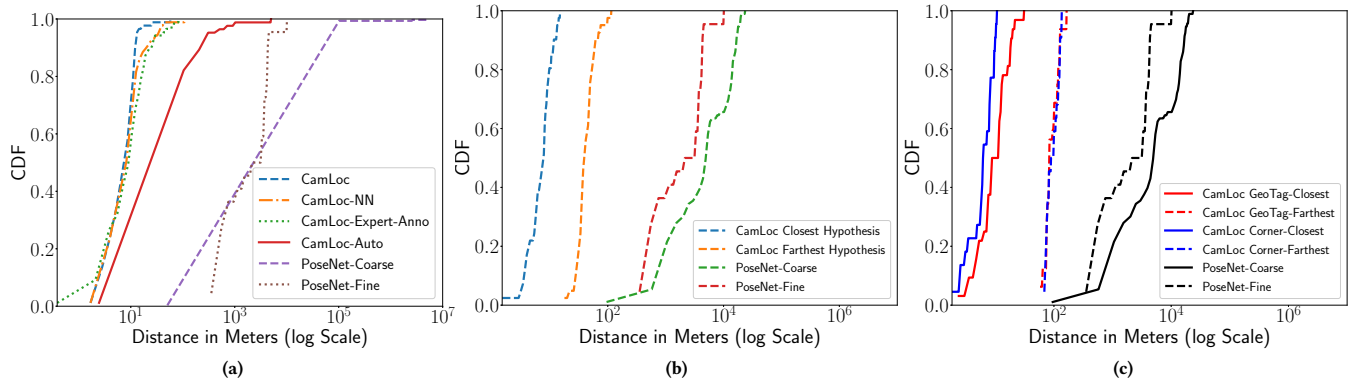


Figure 7: Absolute position error analysis for (a) two pixel-to-GPS mapping based estimation, (b) road corners based estimation, and (c) landmark building based estimation.

location which is less than 10 m away from the camera true position. This number compares well with the absolute localization performance of CamLoc with two known pixel positions.

On the other hand, for the case of mid-point annotations that use the geo-location of the building, the closest candidate is less than 15 meters for approximate 80% of the images and less than 25 meters for 95% of the test cases. This difference arises from the fact that the annotated midpoint may not always correspond to the extracted geo-location. Our compensation for this difference helps, but cannot ensure high accuracy for all images. In both cases, the furthest candidate location is within 100 m of the actual location which is still orders of magnitude better than the performance of the PoseNet-Fine and PoseNet-Coarse.

5.4 Applications

CamLoc’s positioning abilities allows cameras to act as virtual sensors of different types. We now evaluate how well these virtual sensors work.

Virtual Scale and Virtual Clinometer. We select 50 images in our set with marked parking spaces or road dividers (*camera as virtual scale*, §3.3), and annotate two pixels corresponding to lengths ranging from 10 m to 80 m (we obtained the ground truth for these lengths by pinpointing positions on the satellite view). For building height estimation (*camera as virtual clinometer*, §3.3), we handpicked a set of 50 images with visible full buildings of height ranging from 3 m to 55 m (the height ground truth is from Open Street Maps [25]). In Figure 8, we plot the ratio (expressed as a percentage) of the error to the actual dimension. The virtual scale’s error is less than 20% for all of the test cases. On the other hand, the virtual clinometer’s error is less than 25% with 90 percentile and less than 30% with 100 percentile. The larger tail for building height estimation comes from smaller buildings: CamLoc has an absolute error of 1-2 m, which translates to high percentage error in some of the small buildings (our smallest is 3 m).

Virtual Radar. For estimating vehicle speed (*camera as virtual radar*, §3.3), we selected a 10 min worth of video from three of the campus cameras with 100 vehicles with speeds ranging from 10km/hr to 100km/hr (we obtained the groundtruth by pinpointing

the entry and exit positions of the vehicles on the satellite view). For speed estimation, the error (Figure 8) is less than 15% overall and less than 10% at the 80th percentile. The larger error corresponds to estimating the speed of very fast moving vehicles.

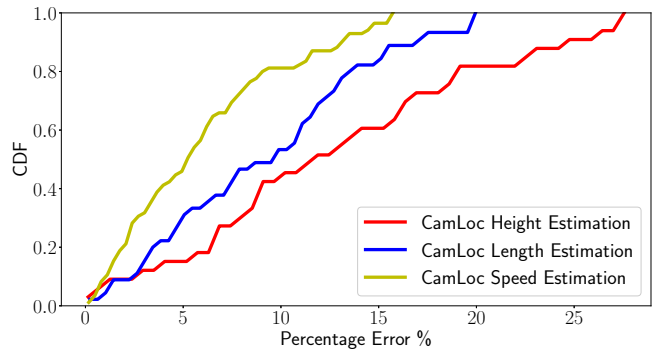


Figure 8: Percentage error for virtual scale, virtual clinometer, and virtual radar.

Virtual guide. To demonstrate the use of the camera as a virtual guide (§4.3), we set up a surveillance camera along a street and asked four volunteers to randomly walk in the camera’s view with an Android phone to log their GPS locations. We applied the method detailed in §4.1 to match the GPS traces with the persons detected on the camera. Our four GPS traces are all correctly matched after a maximum of 2 seconds of bootstrapping time.

Summary. While the virtual sensors are less accurate than the physical ones, they can provide *triage*: for instance, the virtual radar can be used to detect streets with persistent speeders to deploy speed traps, and the virtual clinometer can be used to estimate the approximate height of a skyline for aerial advertising.

5.5 Resource Usage

In this section, we analyze CamLoc in terms of time and resources (compute and human) required for the crucial components.

Annotation Effort. Our dataset includes in total 214 images. We collected 3053 annotations, so on average 14.3 annotations per

image, among which approximate 85% are valid annotations, and 15% were due to spammers on AMT. The median time to finish the annotation for one image is 130.95 seconds or 146.95 person-hours across our entire dataset. For a single camera, annotation is a one-time task, so the required annotation effort required is reasonable.

Run-time of CamLoc with available annotations. We performed a small experiment to estimate the time required to get the results for each image, once we have the annotation. CamLoc takes ≈ 0.41 seconds per image and CamLoc-NN takes ≈ 0.42 seconds per image.

6 Related Work

Camera localization. Most of the work in this area focuses on estimating the 6 degrees of freedom (6-DOF) of a camera that can be subdivided into three broad categories.

Feature Matching based Image Localization: This class of related work mainly focus on identifying the place/view that the image corresponds to. A large class of approaches [26–29] use different image descriptors such as SIFT [30] features, ORB [31] features, bag of visual words [32] or spatial features [33] to compare the query image with a large database of geo-tagged annotated images. Some [34, 35] also compare the image features with the features in Google StreetView dataset. For example, Movshovitz-Attias et al. [36] classify different types of storefronts captured in Google Street View. However, such techniques suffer from two inherent problems: (1) the location of the image is not same as the location of the camera, and (2) the database of images is often sparse and might not contain any matching images [37]. In addition, for surveillance camera images, the quality of the images and the angle of the cameras make it even harder to properly identify and match the image descriptors. Given matched image, the relative camera pose between the query image and the matched image can provide an estimate of the camera’s position This requires the correspondence of at least 5 pixel coordinates in both images [38, 39]. For these reasons, CamLoc uses geometric techniques.

3D model-based localization: The second class of techniques employs a pre-estimated 3D representation of the region of interest for a 2D-3D matching of the features extracted from the query image [8, 40]. Structure from motion methods can provide such a representation [41]. To generate a set of 2D-3D correspondences for such camera relocalization, Shotton et al. [9] propose a regression forests method using RGB-D images; Cavallari et al. [42] extend this by adapting a pre-trained forest to a new scene. However, this class of methods heavily relies on the availability and quality of a 3D map of the environment which is expensive, time-consuming, and often not available in urban environments. In contrast, CamLoc does not require any 3D map of the regions or RGB-D query image for localization.

Neural network based camera pose estimation: PoseNet [6] utilizes a convolutional neural network to regress the camera pose (6-DOF) from a single RGB image. It maps monocular images to a high dimensional space that is linear in pose. This representation allows for full 6-DOF camera pose using regression. Kendall and Cipolla [43] extends PoseNet to incorporate a Bayesian model that

determines the localization’s uncertainty. NetVLAD [44], besides the standard CNN layers, adds a generalized Vector of Locally Aggregated Descriptors (VLAD) [45] layer, which is a popular descriptor pooling method for image retrieval and classification. Kendall and Cipolla [46] showed that PoseNet can improve performance by taking into account geometric loss functions and scene re-projection error. Li et al. [47] present a new angle-based re-projection loss function to solve the problem of the original reprojection loss, enabling neural network training without careful initialization. However, as shown in §5, PoseNet does not generalize well to the diverse set of query images in our dataset. VLocNet [48] and later VLocNet++ [49] use consecutive monocular images and apply multi-task learning (MTL) for learning semantics, 6DoF pose regression, and visual odometry. The performance of all these approaches were mainly tested on the Microsoft 7-Scenes Dataset [50] which is a small indoor dataset and the Cambridge Dataset [51] which is an outdoor dataset consisting of consecutive images from couple blocks taken from a single camera. Like PoseNet, all subsequent extensions are likely to perform poorly due to the lack of generalization. In contrast, the proposed CamLoc system does not rely on any training while generalizing well to images with significant perspective diversity. (As an aside, only PoseNet code is available, so it is the only alternative we evaluate).

Vanishing Point Detection. There exists a large literature on vanishing point detection in the vision community [52–54]. However, accurate vanishing point detection involves grouping of multiple parallel lines in the physical world in order to estimate the respective vanishing point. Detection of such parallel lines in images and grouping them can yield a large number of vanishing points that includes many false positives. Thus, vanishing point detection remains a challenging problem [11] to date. Moreover, we need three mutually orthogonal vanishing points instead of just one vanishing point. While it may be easy to accurately detect 1 to 2 orthogonal vanishing points, in our experience it is much harder and error-prone to detect 3 orthogonal vanishing points in a real world setting. Some approaches use a RANSAC based approach for detecting three orthogonal vanishing points either by relying on known focal length [12] or a known principal point [55]. However, the outputs of these approaches often may not align properly with the three car dimensions selected by our annotators. Our crowdsourcing based vanishing point detection leverages human perception of parallel lines for robust estimation of the vanishing points.

Other Related Work. The work of Xu et al. [56] is complementary to our work that uses computer vision to localize a car on a network of roads by creating a road curvature descriptor. Existing literature also explored localization with respect to both visual and behavior landmarks [57]. Amazon Mechanical Turk (AMT) has been previously used for annotating vision data to obtain ground truth for training [58] and for creating an image ontology database [59]. CrowdSearch [60] is an image search system designed for mobile phones that employs AMT for crowdsourcing and human validation. It combines automated image search with real-time human validation of search results. In CamLoc, we use a similar system [13] for gathering the human annotations.

7 Conclusion

This paper explores the following question: under what conditions is it possible to estimate the location of a camera from a single image taken by the camera? Through a set of carefully designed system components we show that it is possible to use a combination of crowd-sourced annotation from human workers, concepts of vanishing point in projection geometry, the standard dimensions of an object in the image, and the pixel to GPS mapping of two pixels, to uniquely determine the position and height of the camera with less than 12 meters error in 95% of the cases. We also discuss how the pixel to GPS mapping of two pixels can be obtained for two particular cases on real world scenarios. Through an instantiation of our ideas in a tool called CamLoc, we show that our system performs two orders of magnitude better than a state-of-the-art neural network based camera localization system. We further show that Camloc can be used to implement different virtual sensors: virtual scale, virtual clinometer, virtual radar, and virtual guide. Future work with CamLoc involves exploring more complex real-world scenarios, developing techniques to obtain the pixel to GPS mapping for such scenarios, and using multiple images to improve the error performance even further.

References

- [1] ABC Cams. <https://abc7.com/weather/cams/>.
- [2] InseCam. <https://www.insecam.org/>.
- [3] EarthCam. <https://www.earthcam.com/>.
- [4] Johannes Schöning, Antonio Krüger, Keith Cheverst, Michael Rohs, Markus Löchtefeld, and Faisal Taher. Photomap: using spontaneously taken images of public maps for pedestrian navigation tasks on mobile devices. In *Proceedings of the 11th international Conference on Human-Computer interaction with Mobile Devices and Services*, 2009.
- [5] Xiaogang Wang. Intelligent multi-camera video surveillance: A review. *Pattern recognition letters*, 34(1):3–19, 2013.
- [6] Alex Kendall, Matthew Grimes, and Roberto Cipolla. Posenet: A convolutional network for real-time 6-dof camera relocalization. In *The IEEE International Conference on Computer Vision (ICCV)*, 2015.
- [7] A Prusak, O Melnychuk, H Roth, Ingo Schiller, and Reinhard Koch. Pose estimation and map building with a time-of-flight-camera for robot navigation. *International Journal of Intelligent Systems Technologies and Applications*, 5(3/4): 355–364, 2008.
- [8] Torsten Sattler, Michal Havlena, Filip Radenovic, Konrad Schindler, and Marc Pollefeys. Hyperpoints and fine vocabularies for large-scale location recognition. In *Proceedings of the IEEE International Conference on Computer Vision*, 2015.
- [9] Jamie Shotton, Ben Glocker, Christopher Zach, Shahram Izadi, Antonio Criminisi, and Andrew Fitzgibbon. Scene Coordinate Regression Forests for Camera Relocalization in RGB-D Images. In *The IEEE Conference on Computer Vision and Pattern Recognition (CVPR)*, 2013.
- [10] Carsten Rother. A new approach to vanishing point detection in architectural environments. *Image and Vision Computing*, 20(9-10):647–655, 2002.
- [11] Gilles Simon, Antoine Fond, and Marie-Odile Berger. A simple and effective method to detect orthogonal vanishing points in uncalibrated images of man-made environments. In *Eurographics 2016*, 2016.
- [12] J. Bazin and M. Pollefeys. 3-line ransac for orthogonal vanishing point detection. In *2012 IEEE/RSJ International Conference on Intelligent Robots and Systems*, 2012.
- [13] Hang Qiu, Krishna Chintalapudi, and Ramesh Govindan. Satyam: Democratizing groundtruth for machine vision. *CoRR*, abs/1811.03621, 2018. URL <http://arxiv.org/abs/1811.03621>.
- [14] Camera Projection Tutorial. <http://www.cse.psu.edu/~rtc12/CSE486/lecture12.pdf>, 2019.
- [15] Vanishing Point Tutorial. <http://www.cs.princeton.edu/courses/archive/fall13/cos429/lectures/11-epipolar>, 2019.
- [16] Reg G. Willson and Steven A. Shafer. What is the center of the image? *J. Opt. Soc. Am. A*, 11(11):2946–2955, Nov 1994.
- [17] Radu Orghidan, Joaquim Salvi, Mihaela Gordan, and Bogdan Orza. Camera calibration using two or three vanishing points. In *2012 Federated Conference on Computer Science and Information Systems (FedCSIS)*, 2012.
- [18] Simon JD Prince. *Computer vision: models, learning, and inference*. Cambridge University Press, 2012.
- [19] Wei Liu, Dragomir Anguelov, Dumitru Erhan, Christian Szegedy, Scott Reed, Cheng-Yang Fu, and Alexander C Berg. Ssd: Single shot multibox detector. In *European conference on computer vision*, 2016.
- [20] Arsalan Mousavian, Dragomir Anguelov, John Flynn, and Jana Kosecka. 3d bounding box estimation using deep learning and geometry. In *Proceedings of the IEEE Conference on Computer Vision and Pattern Recognition*, 2017.
- [21] Martin A. Fischler and Robert C. Bolles. Random sample consensus: A paradigm for model fitting with applications to image analysis and automated cartography. *Commun. ACM*, 24(6):381–395, June 1981.
- [22] KLT Tracker. https://en.wikipedia.org/wiki/Kanade%27s_Lucas%27_Tomasi_feature_tracker, 2019.
- [23] Aviation Formulary. <http://www.edwilliams.org/avform.htm#LL>, 2019.
- [24] Xiaochen Liu, Yurong Jiang, Puneet Jain, and Kyu-Han Kim. Tar: Enabling fine-grained targeted advertising in retail stores. In *Proceedings of the 16th Annual International Conference on Mobile Systems, Applications, and Services*, 2018.
- [25] Open Street Map. <https://www.openstreetmap.org/>, 2019.
- [26] Mayank Bansal and Kostas Daniilidis. Geometric urban geo-localization. In *The IEEE Conference on Computer Vision and Pattern Recognition (CVPR)*, June 2014.
- [27] B. Zeisl, T. Sattler, and M. Pollefeys. Camera pose voting for large-scale image-based localization. In *2015 IEEE International Conference on Computer Vision (ICCV)*, 2015.
- [28] N. Bhowmik, V. Gouet-Brunet, and B. Soheilian. Cross-domain image localization by adaptive feature fusion. In *2017 Joint Urban Remote Sensing Event (JURSE)*, 2017.
- [29] Anil Armagan, Martin Hirzer, Peter M. Roth, and Vincent Lepetit. Accurate camera registration in urban environments using high-level feature matching. In *British Machine Vision Conference 2017, BMVC*, 2017.
- [30] David G. Lowe. Distinctive image features from scale-invariant keypoints. *International Journal of Computer Vision*, 60(2):91–110, Nov 2004.
- [31] G. Bradski, K. Konolige, V. Rabaud, and E. Rublee. ORB: An efficient alternative to SIFT or SURF. In *2011 IEEE International Conference on Computer Vision (ICCV 2011)*, 2011.
- [32] Oana G Cula and Kristin J Dana. Compact representation of bidirectional texture functions. In *Proceedings of the 2001 IEEE Computer Society Conference on Computer Vision and Pattern Recognition. CVPR 2001*. IEEE, 2001.
- [33] James Philbin, Ondrej Chum, Michael Isard, Josef Sivic, and Andrew Zisserman. Object retrieval with large vocabularies and fast spatial matching. In *2007 IEEE Conference on Computer Vision and Pattern Recognition*. IEEE, 2007.
- [34] Amir Roshan Zamir and Mubarak Shah. Accurate image localization based on google maps street view. In Kostas Daniilidis, Petros Maragos, and Nikos Paragios, editors, *Computer Vision – ECCV 2010*, pages 255–268, 2010.
- [35] D. M. Chen, G. Baatz, K. K  user, S. S. Tsai, R. Vedantham, T. Pylv  dn  dinen, K. Roimela, X. Chen, J. Bach, M. Pollefeys, B. Girod, and R. Grzeszczuk. City-scale landmark identification on mobile devices. In *CVPR 2011*, 2011.
- [36] Y. Movshovitz-Attias, Q. Yu, M. C. Stumpe, V. Shet, S. Arnaud, and L. Yatziv. Ontological supervision for fine grained classification of street view storefronts. In *2015 IEEE Conference on Computer Vision and Pattern Recognition (CVPR)*, 2015.
- [37] Julien Valentin, Matthias Nie  ner, Jamie Shotton, Andrew Fitzgibbon, Shahram Izadi, and Philip HS Torr. Exploiting uncertainty in regression forests for accurate camera relocalization. In *Proceedings of the IEEE Conference on Computer Vision and Pattern Recognition*, 2015.
- [38] D. Nist  r. An efficient solution to the five-point relative pose problem. *IEEE Transactions on Pattern Analysis & Machine Intelligence*, 26(06):756–777, jun 2004.
- [39] W. Zhang and J. Kosecka. Image based localization in urban environments. In *Third International Symposium on 3D Data Processing, Visualization, and Transmission (3DPVT'06)*, 2006.
- [40] Torsten Sattler, Bastian Leibe, and Leif Kobbelt. Efficient & effective prioritized matching for large-scale image-based localization. *IEEE transactions on pattern analysis and machine intelligence*, 39(9):1744–1756, 2017.
- [41] Jan J Koenderink and Andrea J Van Doorn. Affine structure from motion. *JOSA A*, 8(2):377–385, 1991.
- [42] Tommaso Cavallari, Stuart Golodetz, Nicholas A. Lord, Julien Valentin, Luigi Di Stefano, and Philip H. S. Torr. On-the-fly adaptation of regression forests for online camera relocalisation. In *The IEEE Conference on Computer Vision and Pattern Recognition (CVPR)*, 2017.
- [43] A. Kendall and R. Cipolla. Modelling uncertainty in deep learning for camera relocalization. In *2016 IEEE International Conference on Robotics and Automation (ICRA)*, 2016.
- [44] R. Arandjelovic, P. Gronat, A. Torii, T. Pajdla, and J. Sivic. NetVLAD: CNN Architecture for Weakly Supervised Place Recognition. *IEEE Transactions on Pattern Analysis & Machine Intelligence*, 40(06):1437–1451, jun 2018.
- [45] H. J  gou, M. Douze, C. Schmid, and P. P  rez. Aggregating local descriptors into a compact image representation. In *2010 IEEE Computer Society Conference on Computer Vision and Pattern Recognition*, 2010.
- [46] Alex Kendall and Roberto Cipolla. Geometric loss functions for camera pose regression with deep learning. In *The IEEE Conference on Computer Vision and Pattern Recognition (CVPR)*, 2017.

- [47] Xiaotian Li, Juha Ylioinas, Jakob Verbeek, and Juho Kannala. Scene Coordinate Regression with Angle-Based Reprojection Loss for Camera Relocalization. In *ECCV 2018 - Workshop Geometry Meets Deep Learning*, 2018. URL <https://hal.inria.fr/hal-01867143>.
- [48] A. Valada, N. Radwan, and W. Burgard. Deep auxiliary learning for visual localization and odometry. In *2018 IEEE International Conference on Robotics and Automation (ICRA)*, 2018.
- [49] N. Radwan, A. Valada, and W. Burgard. Vlocnet++: Deep multitask learning for semantic visual localization and odometry. *IEEE Robotics and Automation Letters*, 3(4):4407–4414, Oct 2018.
- [50] 7-Scene Dataset. <https://www.microsoft.com/en-us/research/project/rgb-d-dataset-7-scenes/>, 2019.
- [51] Cambridge Dataset. <http://mi.eng.cam.ac.uk/projects/relocalisation/#dataset>, 2019.
- [52] Jana Košecká and Wei Zhang. Video compass. In *European conference on computer vision*, 2002.
- [53] José Lezama, Rafael Grompone von Gioi, Gregory Randall, and Jean-Michel Morel. Finding vanishing points via point alignments in image primal and dual domains. In *Proceedings of the IEEE Conference on Computer Vision and Pattern Recognition*, 2014.
- [54] A. Almansa, A. Desolneux, and S. Vamech. Vanishing point detection without any a priori information. *IEEE Transactions on Pattern Analysis and Machine Intelligence*, 25(4):502–507, April 2003.
- [55] Horst Wildenauer and Allan Hanbury. Robust camera self-calibration from monocular images of manhattan worlds. In *2012 IEEE Conference on Computer Vision and Pattern Recognition*, 2012.
- [56] D. Xu, H. Badino, and D. Huber. Topometric localization on a road network. In *2014 IEEE/RSJ International Conference on Intelligent Robots and Systems*, 2014.
- [57] Yurong Jiang, Hang Qiu, Matthew McCartney, Gaurav Sukhatme, Marco Gruteser, Fan Bai, Donald Grimm, and Ramesh Govindan. Carloc: Precise positioning of automobiles. In *Proceedings of the 13th ACM Conference on Embedded Networked Sensor Systems, SenSys '15*, 2015.
- [58] A. Sorokin and D. Forsyth. Utility data annotation with amazon mechanical turk. In *2008 IEEE Computer Society Conference on Computer Vision and Pattern Recognition Workshops*, 2008.
- [59] Jia Deng, Wei Dong, Richard Socher, Li-Jia Li, Kai Li, and Li Fei-Fei. Imagenet: A large-scale hierarchical image database. In *2009 IEEE Conference on Computer Vision and Pattern Recognition*, 2009.
- [60] Tingxin Yan, Vikas Kumar, and Deepak Ganesan. Crowdsearch: Exploiting crowds for accurate real-time image search on mobile phones. In *Proceedings of the 8th International Conference on Mobile Systems, Applications, and Services, MobiSys '10*, 2010.